ngVLA Memo # 46
Ionized Gas in Globular Cluster Systems

J. M. Wrobel[1] and K. E. Johnson[2]

[1]*National Radio Astronomy Observatory, P.O. Box O, Socorro, NM 87801, USA;* jwrobel@nrao.edu

[2]*Department of Astronomy, University of Virginia, 530 McCormick Road, Charlottesville, VA 22904, USA;* kej7a@virginia.edu

Abstract. Using the Next Generation Very Large Array (ngVLA), we will search for ionized gas in tens of globular cluster (GC) systems out to a distance of 10 Mpc. Constraints on gas in parsec-scale GCs are key to understanding how GC systems and their host galaxies co-evolve. Simulations of gas removal between disk crossings suggest a diversity of gas properties in the Milky Way's GC system. Simulations have yet to examine GC systems hosted by other galaxy types. Our search for ionized gas will motivate and inform such simulations.

1. Scientific Motivation

Constraints on gas in globular star clusters (GCs) are key to understanding how GC systems and their host galaxies co-evolve (Roberts 1988; van Loon et al. 2009, and references therein). As the stars in GCs evolve, they shed gas into the potential wells of the GCs. In the case of the Milky Way, estimates suggest that about 100 to 1000 $M_\odot$ of gas could be built up before being cleared as the GCs cross the disk. Observations do not support these amounts of gas, revealing only about 0.1 $M_\odot$ of ionized gas in the central few parsecs of 47 Tuc and M15 (Pfahl & Rappaport 2001; Freire et al. 2001) and (tentatively) about 0.3 $M_\odot$ of neutral gas in M15 (van Loon et al. 2006). Simulations of gas removal between disk crossings point to diverse gas properties within the Milky Way's GC system (Priestley et al. 2011; Pepe & Pellizza 2013; McDonald & Zijlstra 2015; Pepe & Pellizza 2016).

Observations that enclose the bulk of a GC should provide the most robust constraints on its gas content. A typical GC has a half-light diameter of 4-6 pc (Brodie & Strader 2006). The Milky Way's GCs subtend arcminutes, so some gas inventories require extrapolations, while others risk contamination by discrete sources in front of, within, or behind the GCs, or by the interstellar medium toward the GCs (e.g., Hills & Klein 1973; Knapp et al. 1996; van Loon et al. 2009). In contrast, extragalactic GCs subtend less than an arcsecond beyond the Local Group, making it easier to inventory the bulk of a GC. Also, the entire GC system of a galaxy can be studied, and a variety of galaxy types and environments can be explored. Simulations have yet to consider diverse settings for GC systems.

We have used the US National Science Foundation's Karl G. Jansky Very Large Array (VLA; Perley et al. 2011) to demonstrate the feasibility of a radio search for ionized gas in one nearby GC system (Wrobel & Johnson 2018), and summarize that effort in Section 2. In Section 3 we demonstrate the pivotal role that the Next Generation VLA (ngVLA; Selina & Murphy 2017) will have in searching for ionized gas in tens of GC systems hosted in nearby galaxies. We close, in Section 4, by linking these searches to related studies using facilities contemporary with the ngVLA.

2. Globular Cluster System of M81 with the VLA

Nantais et al. (2011) tabulate 214 probable GCs in M81, a spiral galaxy at a distance of 3.63 Mpc (Freedman et al. 1994). Forty percent are spectroscopically confirmed GCs and the balance are good GC candidates because of their colors and sizes. The 214 GCs have a median 2D half-light diameter of 5.26 pc based upon individual half-light diameters with 40% uncertainties. Our VLA search, at a wavelength of 5.5 cm and spatial resolution of 1.″5 (26.4 pc), captured 206 of the GCs (Wrobel et al. 2016; Wrobel & Johnson 2018). The search yielded 3σ upper limits spanning 3×4.3 to 3×51 μJy beam^{-1} for individual GCs, and 3×0.43 μJy beam^{-1} for the weighted-mean image stack of 206 GCs.

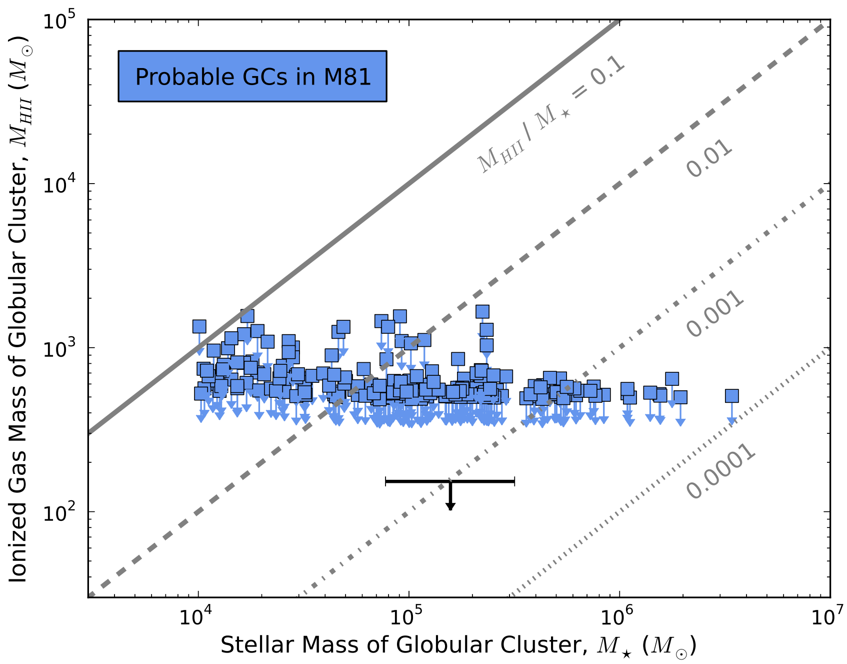

Figure 1. Ionized gas mass, $M_{\rm HII}$, and stellar mass, $M_\star$, for each GC in M81. The grey diagonal lines of constant $M_{\rm HII}/M_\star$ convey ionized-gas-mass fractions. For the stack of 206 GCs, $M_{\rm HII,stack}$ is plotted as a dark line centered at $M_{\star,\rm peak}$. All gas-mass upper limits are at 3σ. From Wrobel & Johnson (2018).

We applied equation (3) from Knapp et al. (1996) to convert the flux-density upper limit for each GC and the GC stack to an upper limit on the ionized gas mass, $M_{\rm HII}$ and $M_{\rm HII,stack}$, respectively. We assumed the gas is optically thin, isothermal as justified by

Scott & Rose (1975) with $T_e \sim 10^4$ K, of uniform density, and spherically distributed with a 3D diameter that is $\frac{4}{3}$ times the median 2D half-light diameter (Spitzer 1987). We adopted the median half-light diameter rather than the poorly-established individual diameters. The stellar mass, $M_\star$, for each GC was retrieved from Wrobel et al. (2016). Using their approach, the peak of the GC luminosity function (Nantais et al. 2011) corresponds to a stellar mass $M_{\star,\mathrm{peak}} \sim 1.6 \times 10^5 M_\odot$.

Figure 1 displays M_{HII} and $M_\star$ for the GCs and shows the stack's $M_{\mathrm{HII,stack}}$ at $M_{\star,\mathrm{peak}}$. From Figure 1, we find: (1) None of the GCs has ionized gas detected with these VLA observations. A typical gas-mass limit is $M_{\mathrm{HII}} < 550\ M_\odot$. Gas-mass fractions, $M_{\mathrm{HII}}/M_\star$, are below about 0.1 at $M_\star \sim 10^4\ M_\odot$ and below about 0.0002 at $M_\star \sim 3.4 \times 10^6\ M_\odot$. (2) From the GC stack, the formal gas-mass limit is about $M_{\mathrm{HII,stack}} < 150\ M_\odot$. Dividing this by the stellar mass peak, the formal gas-mass fraction is below about 0.0009.

Being referenced to the median 2D half-light diameter of the GCs in M81, these ionized gas constraints are resonably robust. They can be improved with deeper radio observations of, and more accurate half-light diameters for, the individual GCs in M81.

3. Globular Cluster Systems with the ngVLA

Following Wrobel et al. (2018), we consider using Band 3 of the ngVLA (Selina & Murphy 2017) to examine GC systems in the local universe. Band 3 has a central frequency of 17 GHz and a bandwidth of 8.4 GHz. We approximate its central wavelength as 2 cm. In the Harris et al. (2013) compilation of GC systems, the distribution of the hosts' distances shows a peak containing tens of galaxies with distances out to 10 Mpc. A typical galaxy's GC system holds several hundred GCs spread over an effective diameter of a few tens of kpcs (Harris 2016; Kartha et al. 2016). Thousands of GCs in total are thus available out to 10 Mpc.

We applied the ionized gas model of Section 2 but now assume that each GC has a 2D half-light diameter of 5 pc (Brodie & Strader 2006). We predict the luminosity at 2 cm as a function of the mass of ionized gas, M_{HII}, in a GC. To minimize beam-broadening corrections, we aim for a tapered, robustly-weighted resolution of 1000 mas. The expected flux densities, S_{2cm}, were then derived for GCs at distances of 3 and 10 Mpc. At these distances the beam-broadening corrections are 1.21 and 1.02, and the spatial resolutions are 14.5 and 48.5 pc. Importantly, we will re-purpose the ngVLA data acquired at a resolution of 100 mas for a search for intermediate-mass black holes (IMBHs) in GC systems (Wrobel et al. 2018). If that search detects a point-like IMBH in a GC, its signal will be removed before tapering to a resolution of 1000 mas for our ionized gas search.

The sloping lines in Figure 2 show how to convert from S_{2cm} to M_{HII} for distances of 3 and 10 Mpc. The vertical lines convey 3σ detections with the ngVLA after integrations of 1, 10 and 100 hours, assuming a tapered, robustly-weighted resolution of 1000 mas (Selina & Murphy 2017). At higher signal-to-noise ratios, the wide frequency coverage could test the optically-thin (flat-spectrum) assumption, as well as provide alerts about steep-spectrum contaminants like background galaxies.

At 3 Mpc the model predicts a flux density of $S_{2cm} = 0.43\ \mu$Jy from 76 $M_\odot$ of ionized gas. The ngVLA can make a 3σ detection with a 10-hour integration and a tapered, robustly-weighted resolution of 1000 mas. The field of view (FOV) of the ngVLA is a circle of diameter 3.4 arcmin (3 kpc) at full width half maximum (Selina

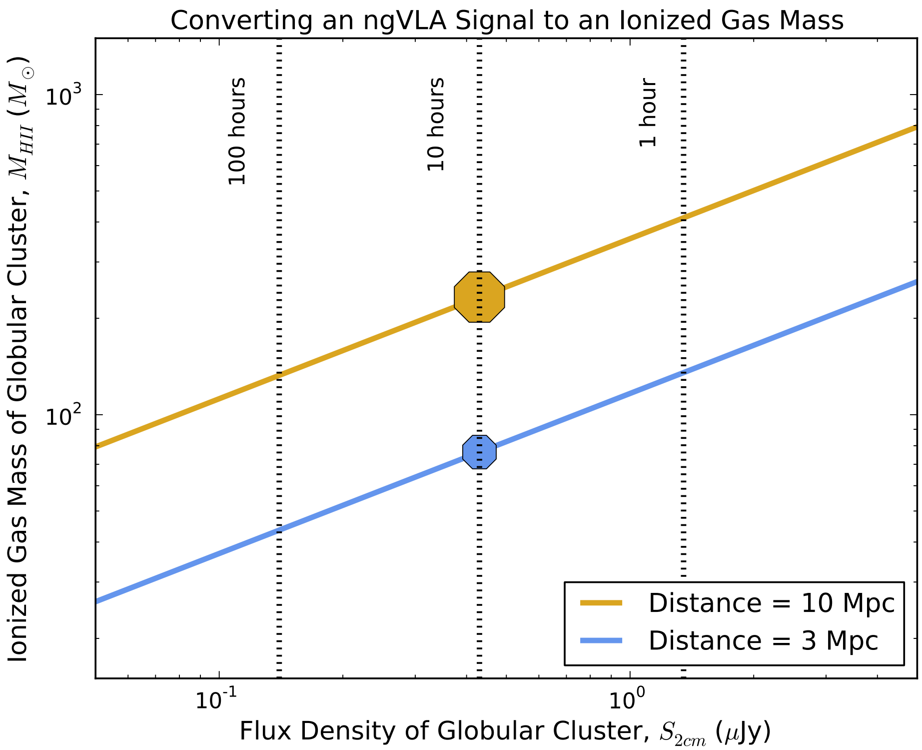

Figure 2. ngVLA signals, S_{2cm}, from ionized gas masses, M_{HII}, in GCs at distances of 3 and 10 Mpc. We assume that the gas is optically thin, isothermal with $T_e \sim 10^4$ K, of uniform density, and spherically distributed with a 3D diameter that is $\frac{4}{3}$ times a 2D half-light diameter of 5 pc. The small and big octagons highlight 3σ mass sensitivities at 3 and 10 Mpc, respectively, for a 10-hour integration. Tens of GC systems have distances out to 10 Mpc, and hold thousands of GCs in total.

& Murphy 2017), so most of a GC system can be encompassed in a modest number of FOVs. Each FOV can simultaneously capture many GCs. Undetected GCs can also be stacked. A stacking performance as for M81 (Section 2) can improve the mass sensitivity by a factor of about three. At 10 Mpc the model predicts a flux density of $S_{2cm} = 0.43$ μJy from 230 $M_\odot$ of ionized gas. The ngVLA can make a 3σ detection with a 10-hour integration and encompass most of the GC system in a few FOVs, with each FOV simultaneously capturing many GCs. Stacking can also be done, and is expected to reach the mass sensitivity mentioned above for an individual GC at 3 Mpc. *In summary, with its sensitivity, bandwidth, spatial resolution, and FOV, the ngVLA at 2 cm will efficiently probe ionized gas masses in tens of GC systems out to a distance of 10 Mpc.*

4. The ngVLA and Its Contemporary Facilities in the 2030s

A key science driver for extremely large telescopes (ELTs) in the 30-m class is to measure, at a distance of 10 Mpc, a black hole mass as low as 100,000 $M_\odot$ by spatially resolving its sphere of influence in its GC host (Do et al. 2014). For example, if the Infrared Imaging Spectrometer (IRIS) [1] on the Thirty Meter Telescope can achieve the diffraction limit of 18 mas at 2 μm, then this approach will yield a sample of IMBHs in GCs out to a distance of 10 Mpc. A valuable by-product of such IRIS studies will be accurate half-light diameters for the GC hosts. We will use those diameters to underpin our ionized gas search, which has implications for the fuel supply responsible for any signatures of accretion onto the IMBHs (Wrobel et al. 2018).

For GCs with declinations south of 10 degrees, the deployment baseline of SKA1-Mid (Dewdney et al. 2015; Borjesson 2017) will offer a spatial resolution of 57 mas at 3.3 cm with uniform weighting. But as only 67 SKA1-Mid antennas will be available at 3.3 cm, the effective collecting area of that telescope will only be about that of the current VLA, which is insufficient for our purposes. This is exacerbated by further sensitivity losses incurred by the need to taper to achieve the desired resolution of 1000 mas

Some of the GC systems in Harris et al. (2013) will need further optical imaging before finding charts are available for all of their GCs. Such images can mostly be acquired with current ground-based telescopes in the 4-m class (e.g., Hargis & Rhode 2014) or 8-m class (e.g., Brodie et al. 2014). Some new images from space-based telescopes might be needed for accurate half-light diameters. For example, the Near Infrared Camera on the *James Webb Space Telescope* will offer spatial resolutions of 80 and 160 mas in its short- and long-wavelength channels, respectively [2].

Acknowledgments. The National Radio Astronomy Observatory is a facility of the National Science Foundation, operated under cooperative agreement by Associated Universities, Inc. K.E.J. is supported by NSF grant 1413231.

References

Borjesson, L. 2017, Notes from the Chair of the SKA Board from the meeting of 718-192017
Brodie, J. P., & Strader, J. 2006, ARA&A, 44, 193
Brodie, J. P., Romanowsky, A. J., Strader, J., et al. 2014, ApJ, 796, 52
Dewdney, P., Turner, W., Braun, R. 2015, SKA-TEL-SKO-0000308
Do, T., Wright, S., Barth, A. J., et al. 2014, AJ, 147, 93
Freedman, W. L., Hughes, S. M., Madore, B. F., et al. 1994, ApJ, 427, 628
Freire, P. C., Kramer, M., Lyne, A. G., et al. 2001, ApJ, 557, L105
Hargis, J. R., & Rhode, K. L. 2014, ApJ, 796, 62
Harris, W. E., Harris, G. L., & Alessi, M. 2013, ApJ, 772, 82
Harris, W. E. 2016, AJ, 151, 102
Hills, J. G., & Klein, M. J. 1973, Astrophysical Letters, 13, 65
Kartha, S. S., Forbes, D. A., Alabi, A. B., et al. 2016, MNRAS, 458, 105
Knapp, G. R., Gunn, J. E., Bowers, P. F., & Vasquez Poritz, J. F. 1996, ApJ, 462, 231
McDonald, I., & Zijlstra, A. A. 2015, MNRAS, 446, 2226
Nantais, J. B., Huchra, J. P., Zezas, A., Gazeas, K., & Strader, J. 2011, AJ, 142, 183
Pepe, C., & Pellizza, L. J. 2013, MNRAS, 430, 2789
Pepe, C., & Pellizza, L. J. 2016, MNRAS, 460, 2542
Perley, R. A., Chandler, C. C., Butler, B. J., & Wrobel, J. M. 2011, ApJ, 739, L1

[1] `https://www.tmt.org/page/science-instruments`

[2] `https://jwst.stsci.edu/files/live/sites/jwst/files/home/instrumentation/technical\documents/jwst-pocket-guide.pdf`

Pfahl, E., & Rappaport, S. 2001, ApJ, 550, 172
Priestley, W., Ruffert, M., & Salaris, M. 2011, MNRAS, 411, 1935
Roberts, M. S., 1988, in IAU Symp. 126, The Harlow-Shapley Symposium on Globular Cluster Systems in Galaxies, ed. J. E. Grindlay & A. G. Davis Philip (Dordrecht: Kluwer), p. 411
Scott, E. H., & Rose, W. K. 1975, ApJ, 197, 147
Selina, R. & Murphy, E. 2017, Next Generation Very Large Array Memo No. 17, ngVLA Reference Design Development & Performance Estimates
Spitzer, L. 1987, *Dynamical Evolution of Globular Clusters* (Princeton, NJ: Princeton University Press), 12ff
van Loon J. T., Stanimirovic, S., Evans A., & Muller, E., 2006, MNRAS, 365, 1277
van Loon J. T., Stanimirovic, S., Putman, M. E., et al. 2009, MNRAS, 396, 1096
Wrobel, J. M., Miller-Jones, J. C. A., & Middleton, M. J. 2016, AJ, 152, 22
Wrobel, J. M., & Johnson, K. E. 2018, RNAAS, 2, 5
Wrobel, J. M., Miller-Jones, J. C. A., Nyland, K. E., & Maccarone, T. J. 2018, ngVLA Memo # 37